Climate Dynamics (1997) 13 : 745–756

Climate Dynamics

Variability in annual mean circulation in southern high latitudes

W. M. Connolley

British Antarctic Survey, High Cross, Madingley Road, Cambridge CB3 0ET, UK

Received: 18 December 1996 / Accepted: 23 May 1997

Abstract. Using a hierarchy of climate models together with observations from gridded analyses, I examine the atmosphere-only and coupled ocean-atmosphere variability in the general circulation for the region south of 40 °S. The variability in mean sea level pressure (MSLP) is well simulated by the coupled models. A complication is that the difference between the two analyses used for verification is comparable to the analysis-model differences. An increase in variability is seen within the hierarchy of model runs although even a model without interannual variations in sea surface temperatures (SSTs) captures most of the observed variability. The temporal variation in MSLP in southern high latitudes has a white spectrum consistent with "random" forcing by weather events and a decoupling from oceanic "integration". In contrast, the spatial pattern of MSLP variability shows large-scale structure that is consistent between observations and various models, even without interannual variation in SSTs. This shows that the models are sufficiently skillful to reproduce the pattern of observed variability and suggests that the pattern of variability is a characteristic of the land-sea distribution and topography.

1 Introduction

The atmospheric circulation shows variability from the smallest to the largest observed scales. This variability is interesting for two overlapping reasons. First, it provides information on the complex interactions between air, sea, sea–ice and land. Secondly, knowledge of natural variation is essential if one is to recognize any superimposed changes due to anthropogenic effects. These latter effects are currently at the borderline of detectability (Houghton et al. 1996) using observations to date and current techniques.

E-mail: wmc@bas.ac.uk, Phone: (01223) 251479, Fax: (01223) 362616

I examine the region south of 40 °S on interannual and longer time scales. I compare observed variability as represented by gridded output from numerical weather prediction (NWP) analyses with a hierarchy of increasingly sophisticated climate models. Once assured that the models are producing an acceptable representation of the atmospheric circulation, one can use model output to probe the relative importance of sea surface temperature (SST) variations, the land-sea distribution and other factors, in generating atmospheric variations.

Various studies (e.g. Kidson 1988; King 1994; Mo and White 1985) have analyzed observed Southern Hemisphere or Antarctic climate variability. Many use station data since gridded analyses are only available for short (approximately 20 y) periods, although Jones and Wigley (1988) attempted to extend the record backwards to 1957 using empirical orthogonal function (EOF) projections onto station data. The longest series of analyses are from the Australian Bureau of Meteorology and are most commonly used. They now cover the approximately 20 y period from 1973. Changes in circulation (principally a deepening of the circumpolar trough and a weakening of the second annual harmonic in mean sea level pressure, MSLP) have been observed since the mid to late-1970s and have been potentially linked to tropical SSTs and, more speculatively, to stratospheric circulation changes due to ozone depletion (Hurrell and van Loon 1994). Longer station records from the Antarctic region (van Loon et al. 1993) confirm these changes in the Australian analyses for areas with actual observations, but also indicate that the 1970s change could be part of longer-term cyclic fluctuations rather than an unique change. Karoly et al. (1996), using EOFs on station data (using both a sparse network between 1901–85 with no Antarctic stations and a denser network for 1955–85), find that the EOF-1 score correlates to the Southern Oscillation Index (SOI) and the EOF-4 score relates to the Trans-Polar Index (Hobart minus Stanley MSLP). However, this latter result may be forced to some extent by the limited station distribution (S. Harangozo, personal communication). The station networks miss much of the variability in the analyses which is over the sea or West Antarctica.

It is only recently that modelling studies of long-term variability have been done using realistic GCMs, due to the computational expense involved. None of these studies specifically address the Southern Hemisphere. An early study by James and James (1989) found red-noise variability peaking at 10–40 y periods in total angular momentum in a simplified GCM. Tett et al. (1997) compared near-surface temperatures from a 1000 y control run from the Hadley Centre coupled GCM to observations. They tested the hypothesis of Hasselmann (1976) that climate variability could be explained as a red-noise autoregressive process, physically representing the integration by the climate system of random weather disturbances. Although this explained much of the variance, there were signs of greater variance at 4 and 8 y timescales consistent with a model ENSO-like behaviour. Manabe and Stouffer (1996) also used a 1000-y GCM run and also concluded that the spectra of sea surface temperature (SST) were in general red in tropical and mid-latitudes. Kawamura et al. (1995) looked at interannual and interdecadal fluctuations in the northern extratropics in the Japan Meteorological Agency model forced with observed SSTs from 1955 to 1988. They found a predominance of interdecadal variability, although they did not quantify this by spectral analysis.

In this study I examine variability in high-southern latitudes, a hitherto ignored area for model variability studies. I compare interannual variability between observations to a hierarchy of climate models of increasing complexity. The model work mentioned has often focused on near-surface air temperature as the primary variable to study, perhaps because of a strong interest in possible global warming. In this paper I focus on MSLP with occasional forays into 500 hPa height, since I am interested in circulation variability. I find that modelled variability increases with model complexity but even the simplest models capture the essential features of the circulation variability. The models reproduce much of the observed variability, but there remain differences between observed variability and that shown by even the most sophisticated model.

2 Data used

Model data are taken from a hierarchy of runs of the Hadley Centre GCM. Observational data come from the Australian Bureau of Meteorology analyses (referred to here as AUSTclim; Le Marshall et al. 1985) and the ECMWF reanalyses (referred to here as ERAclim; ECMWF 1996). Run periods, conditions and names are given in Table 1.

For this study, all data are annual averages and have been interpolated onto a 2.5° by 3.75° latitude–longitude grid, which is the native grid of the climate model. AUSTclim was interpolated to this grid from a 47 by 47 polar stereographic grid. ERAclim was interpolated from a Gaussian grid with a resolution of 1.125° in longitude and approximately 1.12° in latitude.

The land, atmospheric and oceanic components of the GCMs are described by Johns et al. (1996), who describe the run here called CTL, which is forced by constant values for CO_2. Mitchell et al. (1995) describe the SUL run, which is forced by observed CO_2 increases and a parametrisation of observed sulphate aerosols. Both SUL and CTL are preceded by a lengthy ocean spin-up. All the model data used in this study is taken at least a month after the start of the run to avoid any initial atmospheric spin-up. The C20C runs, which are forced by observed SSTs and sea–ice, are described by Rowell (1997). They are an ensemble of six runs (of which only two are used in this work) each initialized with a different atmospheric state. The FIX run, forced by seasonally varying but annually repeated SSTs and sea–ice, is described by Hewitt and Mitchell (1996). The coupled runs (SUL and CTL) have very similar mean climates for the 120 y period considered here (1860–1980) since the climate forcing imposed on SUL only begins to produce noticeable effects by the end of the period.

Table 1. Summary of models and observations used. A: atmospheric model. AO: coupled ocean-atmosphere model

Run name	Type	SSTs and sea–ice	Period
AUSTclim	Analyses	Observed	1973–93
ERAclim	Analyses	Observed	1979–93
FIX	A	Observed repeating	50 year
C20C	A	Observed	1950–89
CTL	AO	Computed	120 year
SUL	AO	Computed	1860–1980

A comparison of NWP climatologies in high-southern latitudes will be the subject of a future study and will not be pursued in detail here. The AUSTclim series is used here chiefly because it is the longest observed series available. However, the series does not seem to be homogeneous. There seems to be a change (principally a deepening of the circumpolar trough and a weakening of the second annual harmonic in MSLP) at approximately 1980. van Loon et al. (1993) conclude that this is caused by a genuine change in atmospheric circulation rather than changes in analysis procedure and data availability. The pattern of variability agrees with the ERAclim for the latter half of the AUSTclim series but shows a pronounced wave-3 pattern in the earlier half. If the change reflects a real change in the nature of the atmospheric circulation then this indicates that a series of 20 y is too short to capture some significant aspects of MSLP variability. Differences in the mean and standard deviation between the climatologies are discussed in later sections.

3 Errors in the mean state

The mean state of a slightly earlier version of the Hadley Centre atmospheric GCM in the south polar region was investigated by Connolley and Cattle (1994). A finding common to other high resolution climate models (Tzeng et al. 1994) is that the circumpolar trough is too deep. Figure 1 shows errors of 8 hPa in SUL compared to ERAclim at 60 °S corresponding to a too-steep gradient in MSLP between 30 °S and 60 °S. The difference of the

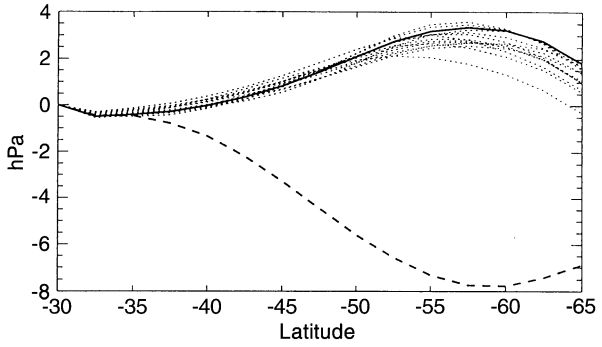

Fig. 1. Differences in zonal mean MSLP between SUL, AUSTclim and ERAclim. *Thick solid line*: AUSTclim (73–93) minus ERAclim (82–94); *thick dashed line*: SUL minus ERAclim (82–94); *thin dotted lines*: differences between AUSTclim and ERAclim for individual overlapping years

models from AUSTclim is slightly less. Other model runs (which share essentially the same atmospheric component) show a nearly identical pattern, providing the run length is long enough to even out fluctuations. The differences between the AUSTclim and the ERAclim are lower (up to 3 hPa) and show a constant bias between years. They are mostly a result of a trough located about 5° poleward in the AUSTclim. I conclude that the mean state of the model, whilst still containing some errors, is good enough to warrant investigation of the variability.

4 Forcing of MSLP by SST and Sea–Ice

The degree to which variations in MSLP are forced by variations in SSTs and sea–ice can be determined by comparing members of the C20C ensemble. This was done by Rowell (1997) who examined the spread of six ensemble members from the ensemble mean. In regions where MSLP is strongly forced by SSTs the ensemble members should be close to each other (measured against interannual variability). Conversely, where there is little direct forcing of MSLP by SSTs the ensemble members for any one year will on average be no closer to each other than they are to other years. The results of Rowell (1997) show that the SST and sea–ice forcing has a strong direct effect in the tropics and little direct effect in the polar regions, except in spring (SON) in the region of the far southeast Pacific. Since the MSLP of the C20C ensemble members in the tropics are close to observations as well as to each other, this result is unlikely to be an artefact of an inadequate model.

Davis (1976) investigated the connections between SST and MSLP in the North Pacific. He found that although MSLP could be hindcast from SSTs on a monthly scale, SSTs had no predictive power for MSLP but rather the reverse, implying that the dominant forcing is atmosphere to ocean. This was revised slightly by Davis (1978) who found a small predictive capability for MSLP (12–20% of the variance) from either MSLP or SST in two seasons, Autumn and Winter. Basher and Thompson (1996) found that SSTs in the New Zealand region lagged air temperature anomalies by half a month, again indicating the dominant forcing is atmosphere to ocean in high latitudes. The feedback of atmospheric temperatures onto ocean temperatures and sea–ice is absent in the C20C runs.

It appears that SST and sea–ice anomalies of a magnitude comparable to observed variations have little discernable impact on MSLP in the polar regions. Much larger perturbations, of course, do have an effect. The reduced sea–ice experiments of Simmonds and Budd (1991) and Mitchell and Senior (1989) show that reductions in sea–ice extent (leading to perturbations in SST of more than 10 °C over a wide area) do lead to significant responses in MSLP. Even these large perturbations tend to produce only locally significant changes in MSLP, and Mitchell and Senior (1989) show that changes in surface roughness (which accompany the removal of sea–ice) are responsible for much of the change in MSLP.

The C20C runs do not include leads in the sea–ice, nor do they include variations in ice thickness which is fixed at 1 m in the Antarctic. Thus a potential source of variability is omitted. However this source is likely to be less important than variations in the ice edge position. Comparing the variability of MSLP in the first 10 y of C20C (when sea–ice data is not available and is imposed from climatology) shows no consistent differences from the last 10 y (in which year-to-year variations are imposed from observations). So, although it is not possible to use these model runs to distinguish the relative roles of SST and sea–ice variability in forcing atmospheric variability, it is likely that problems with the sea–ice are not an important source of error.

5 The standard deviation of MSLP

Zonal mean plots of the standard deviation of annual mean MSLP (Fig. 2) show a general decrease equatorwards. ERAclim and AUSTclim show nearly identical zonal plots up to 55 °S. Between 55 °S and 65 °S ERAclim shows lower variability, but this is caused by the different time periods of the two climatologies. AUSTclim standard deviation for 1979–93 (not shown) is essentially identical to ERAclim. Southwards of 65 °S (not shown) there are large spurious differences caused by different methods used in reducing elevated surface pressures to sea level values. In the zonal mean the models show closer similarities to each other than to the observations. SUL and CTL are very similar to each other and have similar levels of variance to the observations, but a noticeably different structure to the observations with a distinct maximum at 50 °S and a minimum at 60 °S. Two members of the C20C ensemble (arbitrarily labelled 1 and 2) are shown in Fig. 2b compared to the ERAclim. There is a surprisingly large difference between the two ensemble members, although the Mann-Whitney non-parametric test indicates that this is not statistically significant at the 95% level. This difference is somewhat greater than, though comparable to, differences between standard deviation from 40-y sections of SUL or CTL. This further supports the contention that the 20-y period for the AUSTclim is not sufficient for obtaining stable statistics. The FIX run, as

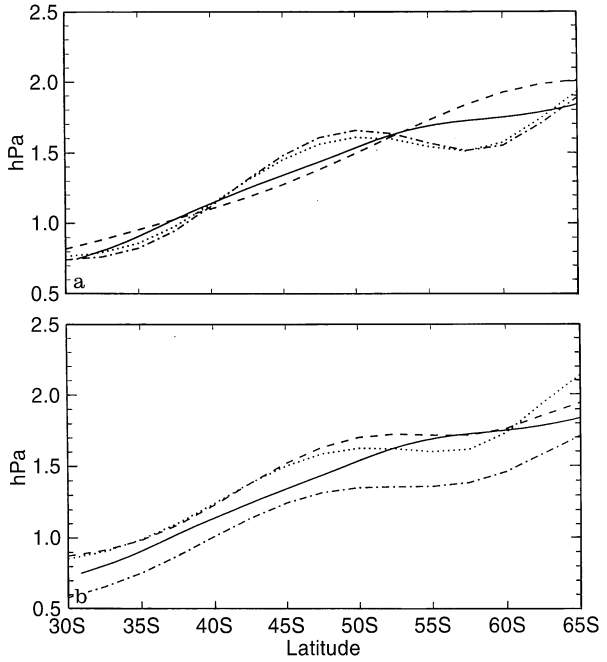

Fig. 2a,b. Zonal mean standard deviation of MSLP from **a** ERAclim (*solid*), AUSTclim (*dash*), SUL (*dotted*) and CTL (*dot-dash*); **b** ERAclim (*solid*), C20C1 (*dash*), C20C2 (*dotted*) and FIX (*dot-dash*)

might be expected, shows the least variance of all with proportionally least in the tropics. As well as lower variability overall, the extrema at 50 °S and 65 °S are less pronounced in FIX.

Examination of maps of the standard deviation (Fig. 3) reveals that differences between the models and observations in the zonal mean hides a quite close pattern similarity. The observations appear to show more "structure" but this is mostly because the models have been averaged over a longer period. Many of the same features recur in the models but are sometimes displaced. The dominant feature in the standard deviation fields for the models and the analyses is a maximum in the standard deviation centred over the Amundsen Sea area and extending into the Bellingshausen and Ross seas, which I call the "West Antarctic pole of variability". This standard deviation maximum is in a data sparse region and so cannot be confirmed or refuted by studies using only station data.

There is a secondary maximum extending from the Ross Sea towards New Zealand in all cases, although the models and observations differ in representing it as a separate maximum or a branch of the pole of variability, respectively. MSLP variations in this region have been linked with ENSO (Trenberth 1976; van Loon and Shea 1987), and the feature is weaker (though still present) in the FIX run. There is another secondary maximum approximately over Kerguelen Island at 80 °E in all fields except FIX.

The "pole of variability" is a robust feature of the analyses and models. It is present, though at a somewhat reduced amplitude, even in the FIX run which has no interannual variation in SSTs or sea–ice. The maximum amplitude of the pole of variability is given in Table 2. Although the analyses mostly have higher values than the models, this may be partly a sampling effect: the range of values in 20-y subseries of CTL and SUL is 2.3 to 3.2 and 2.4 to 3.8 hPa, respectively. The consistency of the pattern even in the absence of SST variations suggests that the location of this feature is largely determined by the land-sea distribution and the topography. Previous studies, looking at factors maintaining the mean circulation, have had mixed conclusions. Quintanar and Mechoso (1995), using a low resolution GCM, found that the amplitude of the zonal wave-1 component of 300 hPa height is largely unaffected by the Antarctic orography and is maintained mostly by wave propagation from lower latitudes. However James (1988) using a non-linear barotropic model found that the features of the flow, including the split-jet structure above New Zealand associated with blocking in that region, could be simulated when the model was forced by Antarctic orography. These studies did not address variability, however. Trenberth (1985) used a form of spectral analysis to examine variability in the 500 hPa height field in the AUSTclim data from 1972 to 1978. This did not show a maximum in the region of the "pole of variability" but was dominated at periods longer than 64 days by maxima in the regions of the New Zealand and Kerguelen secondary maxima. This is confirmed by my own analysis of the period 1973–1978 (not shown). The difference is quite likely to arise from the rather short length of the data used.

The standard deviation from the last 10 y of AUSTclim (Fig. 3e) shows a pattern more similar to the models and to the ERAclim than the standard deviation from the full AUSTclim period (Fig. 3d). This, again, points to problems with the relatively short observational record. The full AUSTclim series (Fig. 3d) appears on visual inspection to have a wave-3 pattern not shown by the models, the second half of the AUSTclim, or ERAclim. More formally, I compute the Fourier components along longitude circles of the standard deviation fields. In the full AUSTclim series wave-3 is the largest component of the MSLP standard deviation field south of 55 °S whereas the ERAclim and models show wave-1 largest at most latitudes. Given the large differences between the observed variability in the different analyses, it is not possible to validate the modelled variability with a high degree of confidence.

The lower level of variability in the FIX run clearly shows the importance of SST variations in generating interannual variability. However, the large fraction of variability that is present (over 80% of that in SUL south of 40 °S) shows that a certain measure of interannual variability is present even in the absence of SST forcing. This may come from intrinsic atmospheric long-time scale variability (James and James 1989) or from forcing by interannual variations in land–surface processes which are not constrained. The latter have been found to be important for precipitation variations over land (Koster and Suarez 1995) although their influence over distant oceanic regions is unclear. This could be determined by a run similar to FIX but with a fixed annual cycle of land hydrology; such a run remains to be done.

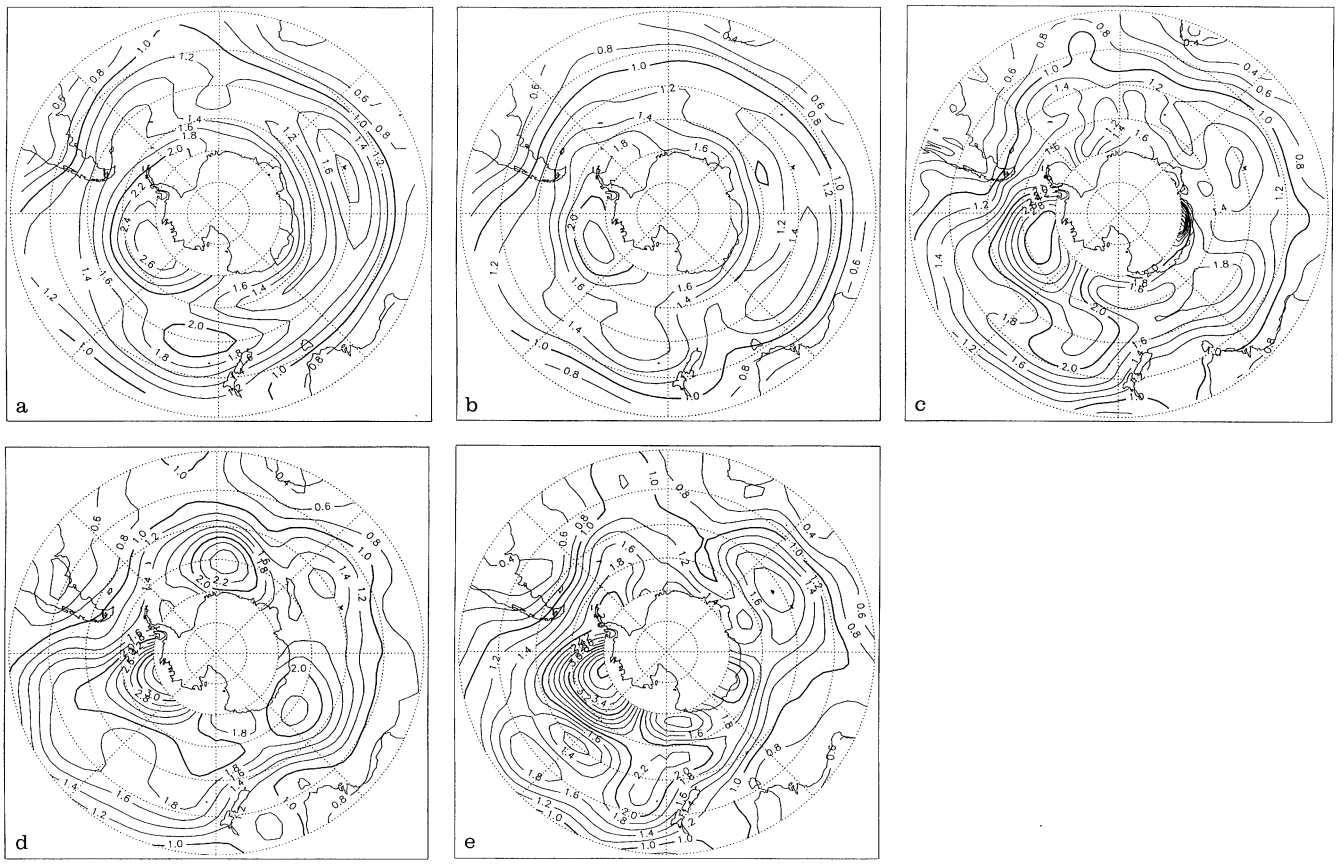

Fig. 3a–e. Standard deviation of MSLP from **a** SUL, **b** FIX, **c** ERAclim, **d** AUSTclim (73–94) and **e** AUSTclim (84–93). Contour interval 0.2 hPa; *1, 2* and *3 hPa* contours in *bold*

Table 2. Maximum amplitude (hPa) of the standard deviation of annual mean MSLP in the Amundsen Sea area for analyses and models

Run:	AUSTclim	ERAclim	SUL	CTL	FIX	C20C1	C20C2
SD:	3.5	3.2	2.8	2.9	2.3	3.4	2.9

One can also compare the models to observations at a few locations with long records. I use the joint Orcadas/Signy (60.7 °S, 45.6 °W) record which begins in 1904 and the Faraday (64.3 °S, 65.3 °W) record which begins in 1944, taken from the database of Jones and Limbert (1987) and updated at the British Antarctic Survey to include data up to 1994. Table 3 gives the standard deviations of MSLP at the station locations from observations, NWP analyses and models. The slight increase in standard deviation in the ERAclim compared to AUSTclim and station observations is because the ERAclim covers a later period than AUSTclim, and variability has increased somewhat in this period. The models have higher standard deviations than the observations, substantially so in the case of Faraday. Figure 3 shows that this is largely due to the West Antarctic pole of variability, which extends further over the Peninsula in the models than in the observations.

Table 3. Standard deviation (hPa) of annual average MSLP at Faraday and at Orcadas/Signy, from station observations, NWP analyses and models

	Obs	AUST clim	ERA clim	SUL	CTL	FIX	C20C 1	C20C 2
Faraday	1.4	1.4	1.7	2.1	1.9	1.8	2.4	2.1
Orcadas/ Signy	1.4	1.4	1.5	1.7	1.6	1.7	1.7	1.6

6 Empirical orthogonal function analysis

I use unrotated empirical orthogonal functions (EOFs) to examine the structure of the variation in annual average MSLP. Rotated EOFs are claimed to have four major advantages: the rotated EOFs suffer less from domain shape dependence, subdomain instability, sampling errors and "faithfulness to relationships embedded in the covariance matrix" (Richman 1983). In this case, I have checked that the EOFs do not suffer from the first two problems: this may be linked to the large size of the domain. For the third problem, I use the North et al. (1982) criterion outlined later to ensure that sampling errors are contained. Since I have no reason to expect the

data fields to show "simple structure" (Richman 1983) there is no reason to expect the rotated EOFs to be more faithful to the data than the unrotated EOFs. When the first 10 EOFs are Varimax-rotated together the rotated EOFs display implausible physical patterns with a tendency for large values in only one area of each EOF. This is less true when only 4 EOFs are rotated, but would introduce the unwelcome complication of deciding how many EOFs to rotate.

A grid from 30 °S to 70 °S was used for the EOF analysis. The rule of thumb of North et al. (1982) was used to ensure that the EOFs were at least well resolved with respect to sampling errors. This states that the sampling error, ε, associated with an eigenvalue, E, is approximately $E\sqrt{(2/n)}$ where n is the number of samples used to construct the covariance matrix. If the eigenvalue separation is less than or comparable to this the eigenvalue problem may be degenerate and the solutions may produce a mixing of the EOFs. I judge neighbouring eigenvalues E_i and E_{i+1} to be non-degenerate if $E_i \pm \varepsilon_i$ and $E_{i+i} \pm \varepsilon_{i+1}$ do not overlap. By this criterion the first model EOF is always distinct but the observed (AUSTclim and ERAclim) is not. The second EOF is not distinct. In the following I shall generally only consider the first EOF.

When using EOF analysis one has to consider whether use of the covariance or correlation matrix is appropriate. The former gives greatest prominence to areas of high variability and is perhaps most appropriate in this case. The latter is appropriate when variables of widely differing variability are compared. Both covariance and correlation matrix analyses were tried. Patterns from both are similar but the former gives slightly greater prominence to the Amundsen Sea area, the area of greatest variability. The area-weighted correlation between the covariance and correlation EOF-1 varies between 0.80 (AUSTclim) and 0.99 (SUL and CTL), and for EOF-2 between 0.55 (AUSTclim) and 0.82 (CTL). Higher EOFs show much weaker correlations. The correlations between the EOF projections is even stronger, above 98% in all cases for EOF-1 except for ERAclim (0.85). This suggests that both are tracking the same structures in the data. If covariance or correlation is not explicitly mentioned, conclusions following are true for either.

For the models the first EOF, on average accounting for 36% of the covariance matrix variance and 24% of the correlation variance, shows an approximately zonal pattern with a change from positive to negative values at approximately 55 °S. EOF-1 of SUL is shown in Fig. 4a and is very similar to EOF-1 of CTL and other models; see Table 4. This pattern is similar to that found by Mo and White (1985) from a correlation-matrix EOF analysis of summer and winter periods in AUSTclim between 1972 and 1981. In the current work, EOF-1 from AUSTclim shows a strong wave-3 pattern (Fig. 4b, Fig. 6c) not present in the models or previous studies. However, the AUSTclim series is short and the EOF not formally distinct; the EOF from the last 15 y of the series only produces a pattern very similar to the models. The first EOF from the full AUSTclim series is, however, similar to the EOF-2 from the Mo and White (1985) analysis. The latter difference may be because Mo and White (1985) looked at summer and winter separately and used 500 hPa height. It should also be noted that the eigenvalues of the Mo and White (1985) study were not distinct according to the North criterion, perhaps due to their shorter time period, so their eigenvectors could be subject to degeneracy. EOF-1 in AUSTclim accounts for less variance than in the models, only 26% on the covariance and 20% in the correlation; the first EOF is not strictly distinct according to the North criterion. This is partly because the AUSTclim has a rather short series, 21 y, available for analysis, but it also suggests that the AUSTclim variance may be more complex than the model variance. Kawamura et al. (1996) found that the leading EOF mode for the northern extratropic 500 hPa height field explained only 16% of the modelled and 9% of the observed variance. Thus, their observed EOF explained less variance than their modelled EOF, as I find. However, comparing the Kawamura et al. variance of the northern extratropics to the variance I find in the southern extratropics, the amount explained is much less, possibly indicating more coherent variability in the southern extratropics.

The EOF-2 pattern is less constant between the models than the EOF-1 (Table 4). There is agreement between the models with varying SSTs, but no correlation with the analyses; this may be because the short length of series of both analyses leads to a poor resolution of the higher

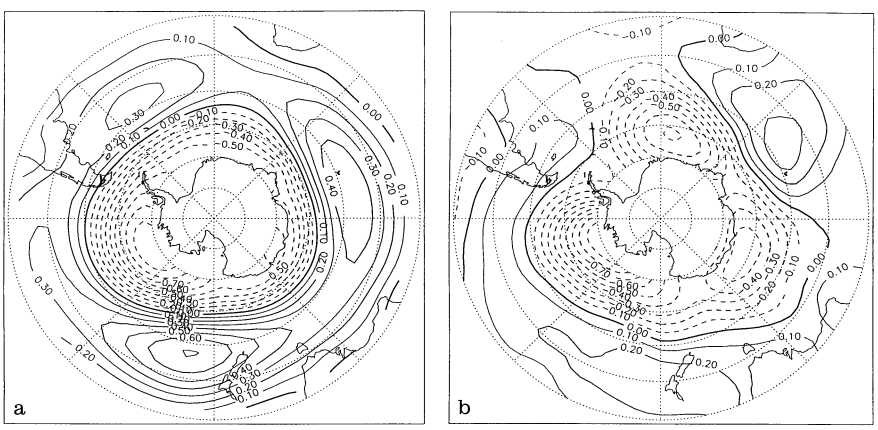

Fig. 4a,b. EOF-1 from the covariance matrix for **a** SUL and **b** AUSTclim. The scaling is arbitrary. *Negative contours dashed, zero contour bold*

Table 4. Area-weighted spatial correlations between EOFs from SUL and other sources

Run	EOF-1	EOF-2
CTL	0.98	0.67
C20C1	0.98	0.55
FIX	0.95	0.13
ERAclim	0.89	0.29
AUSTclim	0.77	0.19

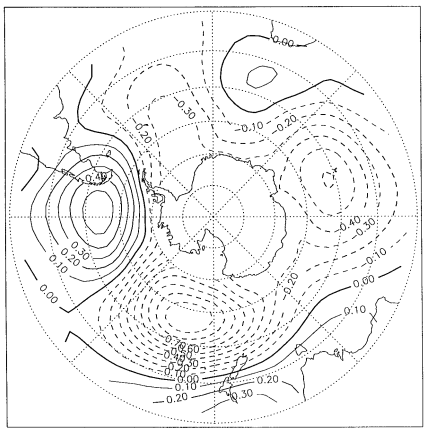

Fig. 5. EOF-2 from the covariance matrix for SUL. The scaling is arbitrary. *Negative contours dashed, zero contour bold*

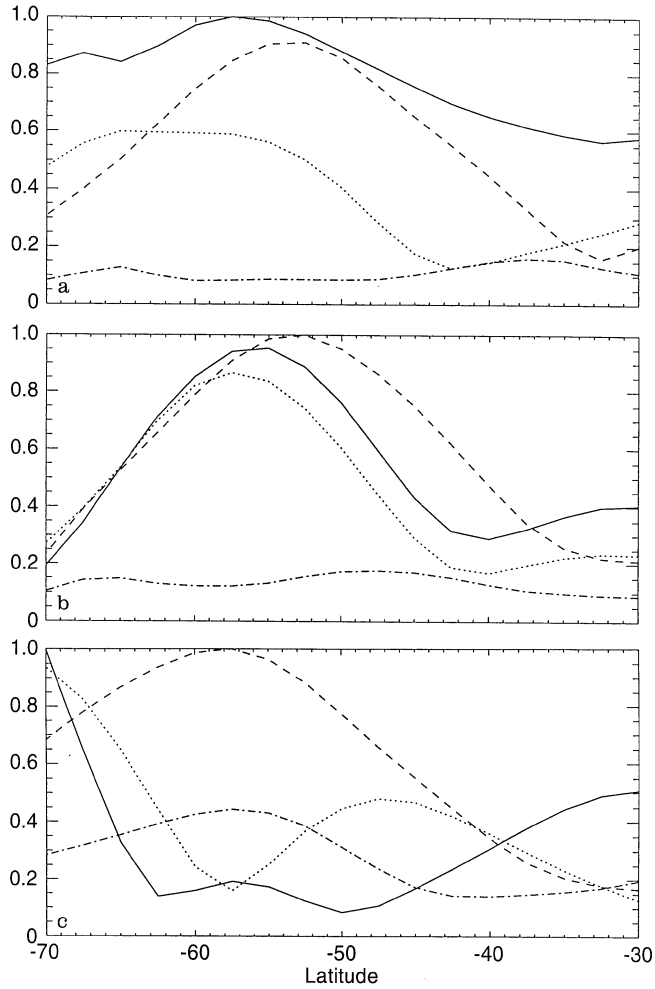

Fig. 6a–c. Fourier decomposition (first 4 modes; zonal mean, wave-0 suppressed) along latitude circles of **a** SUL EOF-1, **b** SUL EOF-2, **c** AUSTclim EOF-1. *Solid*: wave-1; *dotted*: wave-2; *dashed*: wave-3; *dot-dashed*: wave-4. The vertical scale is arbitrary

modes of variability. The SUL EOF-2 (Fig. 5), although not formally distinct, shows a dipole pattern between the "pole of variability" area and the subsidiary variability maximum south of New Zealand. It shows a strong visual wave-3 pattern. This is confirmed by a Fourier decomposition along latitude circles (Fig. 6), which also shows that almost all zonal variance in SUL EOFs 1 and 2 occurs in the first 3 wave numbers.

The correlation between EOF-1 of the AUSTclim 500 hPa height field and the MSLP field is 0.89 and the correlation of the EOF-1 projection between the two is 0.90. For SUL, the values are 0.94 and 0.98 respectively. Thus circulation variations on the large scale are largely barotropic in both models and observations. Higher EOFs show substantial correlations between MSLP and 500 hPa height but with some mixture between EOFs. This is to be expected in view of the possibility of sampling errors due to possibly degenerate EOFs.

7 Spectral analysis

I have shown that there is considerable spatial coherence in the circulation variability on annual time scales. In this section I consider the temporal characteristics of variability by examining power spectra. I look at the spectra of the EOF-1 time series and also the spectra from two locations (Orcadas/Signy and Faraday) where models can be compared to long observational records. EOF-1 represents a large fraction of the MSLP variance and represents changes present over a large area, so its projection onto the MSLP field is a good circulation index. Also, it is strongly correlated to MSLP variations at points in the Bellingshausen sea: at 65 °S, 110 °W the correlation in SUL is 0.89 and in AUSTclim it is 0.77. For calculating projections the EOF is scaled to have unit area-averaged standard deviation. Spectra are computed by FFT after first detrending the time series (if a significant trend exists) and windowing as in Hamming (1977). The spectra are smoothed by a running mean of width approximately 5% of the length of the series. For constructing confidence limits (Gottman 1981) I fit a white or red noise spectrum to the spectrum according to whether the lag-1 autocorrelation coefficient is significantly different from zero. In all cases described, the best fit is to a white noise spectrum.

James and James (1989) examined low-frequency variability in a simplified atmospheric GCM. They found a red spectrum in large-scale variability in 100-y runs. In a longer run (684 y) with fixed solsticial forcing it appeared that the spectrum had peaked in approximately the 10–40 y band. Other studies, usually looking at SSTs and

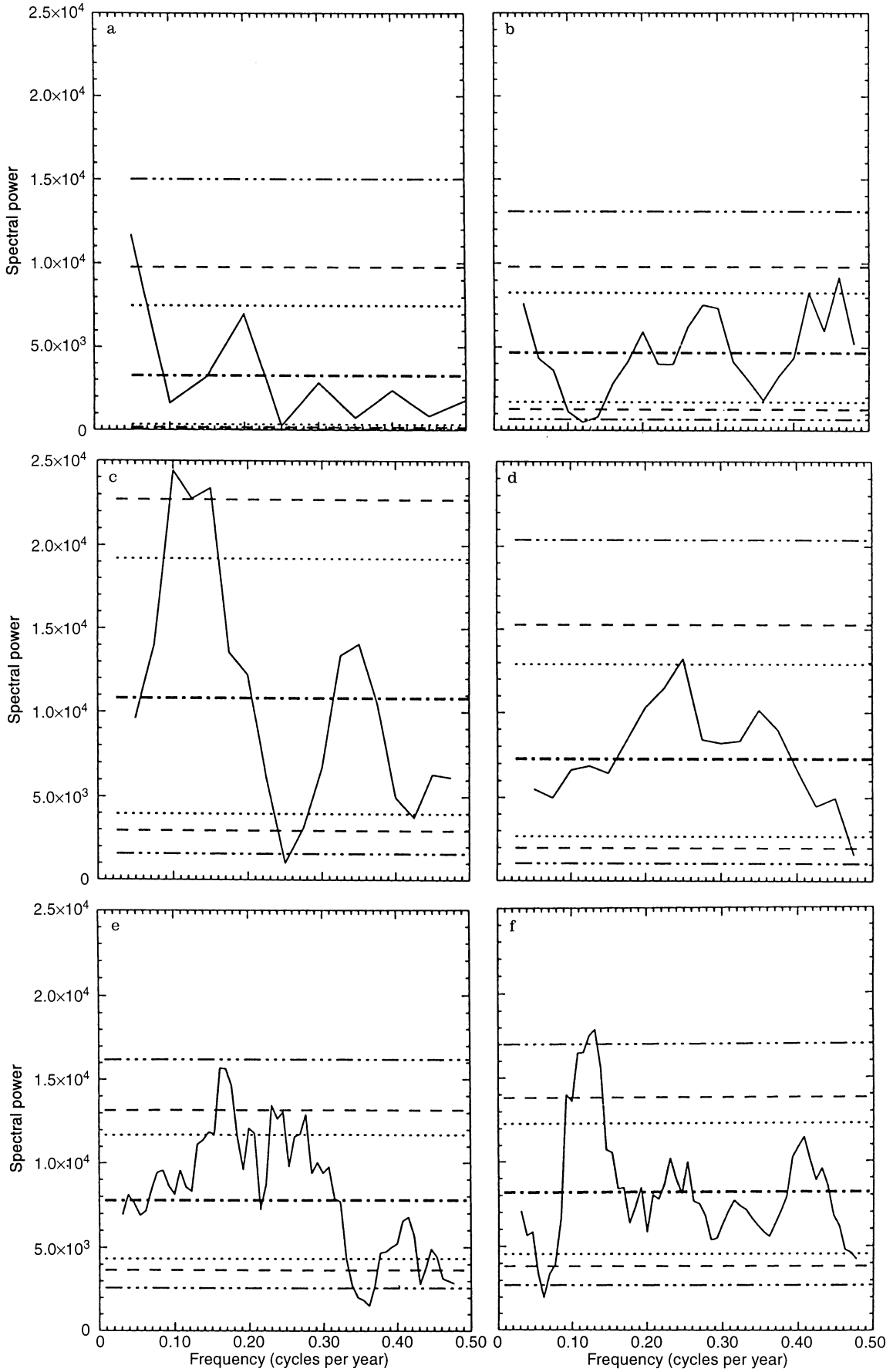
a
b
c
d
e
f
Spectral power
2.5×10^4
2.0×10^4
1.5×10^4
1.0×10^4
5.0×10^3
0
0.10
0.20
0.30
0.40
0.50
Frequency (cycles per year)

generally in the tropics, generally find a red spectrum. An exception is Davis (1976) who found a white spectrum in North Pacific MSLP but a red spectrum in the SST. In the runs used here there is no clear evidence for a red spectrum. Looking at projections of EOF-1 onto the data, lag-1 autocorrelations are not significantly different from zero. The spectra appear to show peaks within a white spectrum rather than a red spectrum. This may seem something of a surprise, until we recall the results of Rowell (1997) mentioned in Sec. 2 which show little forcing of MSLP by SSTs in the polar regions. If the Hasselmann explanation for a red spectrum is correct (ocean integration of local weather "noise") then one would expect a white spectrum in the polar regions, since MSLP variations are largely decoupled from SST variations.

The lagged correlations of the EOF projections show no significant values and therefore the spectra are judged to be best fitted as "white". The AUSTclim (Fig. 7a) shows no peaks except at lowest frequency. Because of the shortness of the record it is not possible to judge the significance of this directly, but comparisons with station data (later) indicate that the AUSTclim spectrum is not representative of longer periods. FIX and C20C2 show no clearly significant peaks, although C20C1 has a possibly significant peak at 8 y. SUL has a peak at 8 y periodicity, and CTL at 6 y, but while these peaks are nominally significant at, respectively, 99% and 95% a certain number of "false positives" are to be expected from the statistical test. Furthermore, the SUL and CTL peaks are not fully robust, in that 60-y subseries do not always show these peaks. However, taken together, the runs with varying SSTs show a tendency towards peaks in the 6–8 y range that might be significant if they could be linked to a physical mechanism. Tett et al. (1997) shows that an extension of CTL from the 120 y used in this study to 1000 y has a peak in global mean SST at 8 y periodicity, but that whilst this peak is individually significant the overall fit to a red spectrum is not significantly worse than could have occurred by chance.

It is useful to compare spectra of MSLP at point locations as well as the more general index provided by the EOF-1 coefficients. I use the 90 y joint Orcadas/Signy (60.7 °S, 45.6 °W) record which begins in 1904 and the 50 y Faraday (64.3 °S, 65.3 °W) record which begins in 1944. The spectrum of the Faraday station record (Fig. 8a) shows just significant peaks at 8 and 4 y; the former is characteristic of the first half of the record; the latter of the last 30 y and is the only peak in the AUSTclim (Fig. 8b). SUL, CTL and FIX (not shown) have no significant peaks in the spectra when interpolated to the station locations. C20C2 has a peak in the 4–5 y range but C20C1 does not.

Fig. 7a–f. Spectra of EOF-1 projections. **a** AUSTclim, **b** FIX, **c** C20C1, **d** C20C2, **e** CTL, **f** SUL. SUL and CTL spectra have been smoothed with a running mean of width 7, FIX and C20C by width 3 and AUSTclim is unsmoothed. *Horizontal lines* indicate 90% (*dotted*), 95% (*dashed*) and 99% (*dot-dashed*) confidence levels for significance against theoretical white noise spectrum (*thick line*) appropriate to the smoothed spectrum. Spectra are scaled so that the power at each frequency is the variance of a white-noise process with that power

I noted in Sec. 3 that the modelled variance at Faraday was higher than observations, which is reflected in the higher spectral power of C20C in Fig. 8c,d. My explanation for this, an extension of the "West Antarctic pole of variability" northwards in the model, suggests that the modelled Faraday point is experiencing a different climatic regime to the observations. Therefore, one would not expect close similarity in the modelled and observed spectra. Orcadas is less affected by this problem and observed station records (Fig. 9a) and SUL and CTL models (Fig. 9c,d) agree in that the spectrum shows little evidence of peaks. AUSTclim, however, shows a clear peak at 5 y, which is present in the station data if the analysis is restricted to the last 20 y of the record. These longer station records seem to show that, as well as the apparent change in the circulation recorded in the AUSTclim analyses in the early 1980s, the statistics of annual mean circulation have not been constant throughout this century.

8 Conclusions

I have examined modelled and observed variability in the general circulation for the region south of 40 °S. Differences in the general degree of variability in MSLP simulated by the coupled models (as measured by the standard deviation field) compared to the observations seem as small or smaller than differences in the simulation of the mean field. This is an important development because past model verification in the Antarctic (e.g. Connolley and Cattle 1994) considered only the mean state. An important complication is that the difference between the two analyses used for verification is comparable to the analysis-model differences. A separate study will address the intercomparison of observational analyses.

An increase in variability is seen between FIX and higher-level models, although even FIX captures much of the observed variability. This (supported by differences between C20C runs) suggests internally generated variability within the atmosphere (or land–surface scheme) is responsible for much model variability in the study region. This appears to be characteristic of the polar regions (Rowell 1997) but is certainly not true of the tropics. No clear differences in variability are evident between the C20C and coupled runs. Nor is there much evidence of oceanic "reddening" of the spectrum from the coupled runs, and only marginal evidence of spectral peaks. Empirical orthogonal function analysis shows that the first EOF accounts for a large fraction of the variance (typically 36% for the models and 26% for AUSTclim),which is higher than in the Northern Hemisphere. The pattern is mainly zonal, with a maximum in the region of the "West Antarctic pole of variability" where the standard deviation is highest. As with the standard deviation, the EOF pattern shows consistency, even between models with and without interannual variation in SSTs.

The clearest result to emerge from this study is that the temporal variation in MSLP in southern high latitudes (measured by indices of large-scale circulation or pressure at selected points) has a white spectrum consistent with "random" forcing by weather events and a decoupling

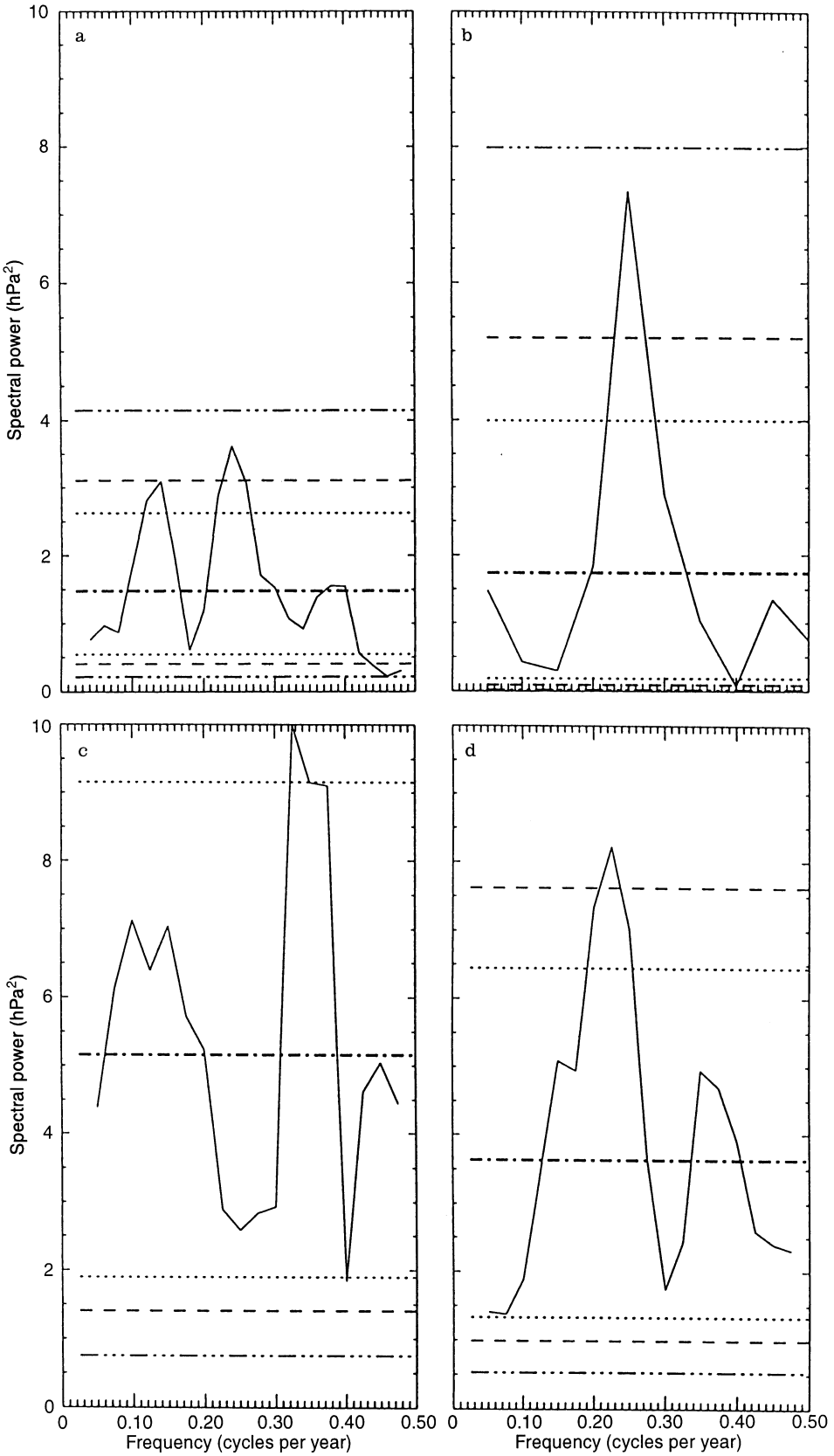

Fig. 8a–d. Spectra of annual mean MSLP at Faraday (64.3 °S, 65.3 °W) **a** station observations and **b** AUS-Tclim, **c** C20C1 and **d** C20C2 interpolated to the station location. Explanation of lines and scaling as for Fig. 7

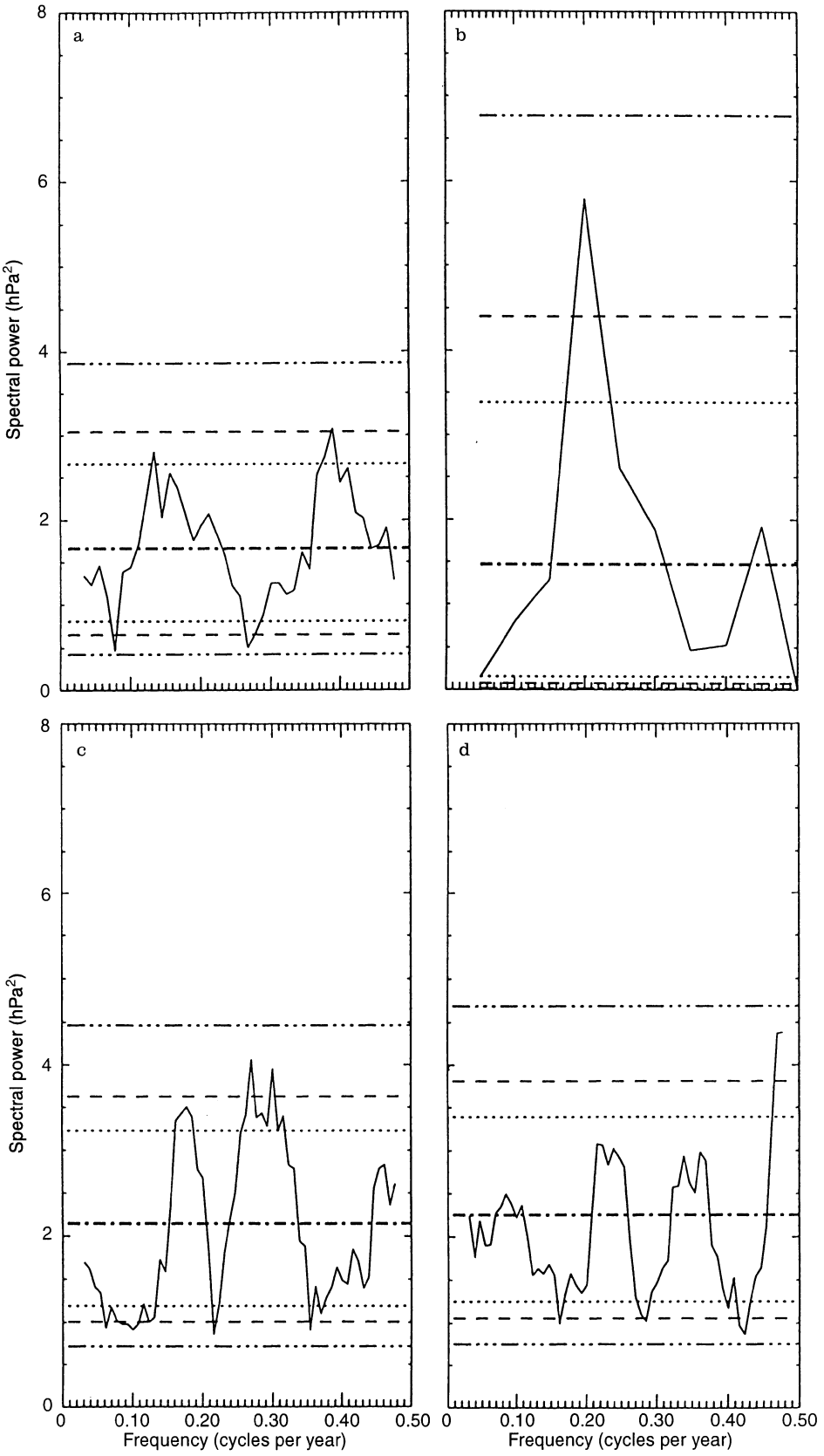

Fig. 9a–d. Spectra of annual mean MSLP at Orcadas/Signy (60.7 °S, 45.6 °W) **a** station observations and **b** AUSTclim, **c** CTL and **d** SUL interpolated to the station location. Explanation of lines and scaling as for Fig. 7

from oceanic "integration" (Hasselmann 1976). However, the spatial variation of MSLP shows large-scale patterns that are consistent between observations and various models. The general spatial pattern of interannual variation in MSLP is similar between observations and models (even without interannual variation in SSTs). This shows that the models are sufficiently skillful to reproduce the pattern of observed variability and suggests that the pattern of variability is a characteristic of the land–sea distribution and topography, rather than forced by any specific variation in SSTs or sea–ice. An interesting extension to this work would be to run a series of experiments to determine precisely which elements of these boundary conditions is important in influencing the pattern of variability.

Acknowledgements. I thank my colleagues S. Harangozo and J. King for valuable discussions, and the Hadley Centre for permission to use their model data for this study. In particular: C. Hewitt (FIX), D. Rowell, C. Folland, A. Renshaw, D. Sexton and J. Davies (C20C; DoE contract PECD3/12/37 and CEC contract EV5V-CT92-0121), T. Johns (and group members) for CTL and SUL. AUSTclim data were provided by the Australian Bureau of Meteorology and processed by S. Colwell. ERAclim data from the ECMWF reanalysis project were provided by the British Atmospheric Data Centre.

References

Basher RE, Thompson CS (1996) Relationship of air temperatures in New Zealand to regional anomalies in sea surface temperature and atmospheric circulation. Int J Climatol 16:405–426

Connolley WM, Cattle H (1994) The Antarctic climate of the UKMO unified model. Ant Sci 6:115–122

Davis RE (1976) Predictability of sea surface temperature and sea level pressure anomalies over the north pacific ocean. J Phys Ocean 6:249–266

Davis RE (1978) Predictability of sea level pressure anomalies over the north Pacific ocean. J Phys Ocean 8:233–246

ECMWF (1996). The ECMWF Re-analysis (ERA) Project. ECMWF newsletter #73, available from ECMWF, Shinfield Park, Reading, RE2 9AX, UK

Gottman JM (1981) Time-series analysis. Cambridge University Press, Cambridge, UK

Hamming RW (1977) Digital filters. Prentice Hall, Englewood Cliffs, New Jersey, p 179

Hasselmann K (1976) Stochastic climate models. Part I. Theory. Tellus 28:473–485

Hewitt CD, Mitchell JFB (1996) GCM simulations of the climate of 6k BP: mean changes and interdecadal variability. J Climate 9:3505–3529

Houghton JT, Meira Filho LG, Callander BA, Harris N, Kattenberg A, Maskell K (1996) Climate change 1995: the science of climate change. CUP, Cambridge, UK

Hurrell JW, van Loon H (1994) A modulation of the atmospheric annual cycle in the Southern Hemisphere. Tellus 46:325–338

James IN (1988) On the forcing of planetary scale Rossby waves by Antarctica. Q J R Meteorol Soc 114:619–637

James IN, James PM (1989) Ultra-low-frequency variability in a simple atmospheric circulation model. Nature 342:53–55

Johns TJ, Carnell RE, Crossley JF, Gregory JM, Mitchell JFB, Senior CA, Tett SFB, Wood RA (1997) The second Hadley Centre coupled ocean-atmosphere GCM: model description, spinup and validation. Clim Dyn 13:103–134

Jones PD, Limbert DWS (1987) A data bank of Antarctic surface temperature and pressure data. Office of energy research, Rep TR038. United States Department of Energy, Washington

Jones PD, Wigley TM (1988) Antarctic gridded sea level pressure data: an analysis and reconstruction back to 1957. J Climate 1:1199–1220

Karoly DJ, Hope P, Jones PD (1996) Decadal variations of the southern hemisphere circulation. Int J Climatol 16:723–738

Kawamura R, Sugi M, Sato N (1996) Interdecadal and interannual variability in the Northern extratropical circulation simulated with the JMA global model. Part I: wintertime leading mode. J Climate 8:3006–3019

Kidson JW (1988) Indices of the Southern Hemisphere zonal wind. J Climate 1:183–194

King JC (1994) Recent climate variability in the vicinity of the Antarctic Peninsula. Int J Climatol 14:357–369

Koster RD, Suarez MJ (1995) Relative contributions of land and ocean processes to precipitation variability. J Geophys Res 100:13775–13790

Le Marshall JF, Kelly GAM, Karoly DJ (1985) An atmospheric climatology of the Southern Hemisphere based on ten years of daily numerical analyses (1972–1982): I overview. Aust Meteorol Mag 33:65–85

Manabe S, Stouffer RJ (1996) Low-frequency variability of surface air temperature in a 1000-year integration of a coupled atmosphere-ocean-land surface model. J Climate 9:376–393

Mitchell JFB, Senior CA (1989) The antarctic winter; simulations with climatological and reduced sea–ice extents. Q J R Meteorol Soc 115:225–246

Mitchell JFB, Johns TC, Gregory JM, Tett SFB (1995) Climate response to increasing levels of greenhouse gases and sulphate aerosols. Nature 376:501–504

Mo KC, White GH (1985) Teleconnections in the Southern Hemisphere. Mon Weather Rev 113:22–37

North GR, Bell TL, Cahalan RF, Moeng FJ (1982) Sampling errors in estimation of empirical orthogonal functions. Mon Weather Rev 110:699–706

Quintanar AL, Mechoso CR (1995) Quasi-stationary waves in the Southern Hemisphere. Part II: generation mechanisms. J Climate 8:2673–2690

Richman MB (1983) Rotation of principal components. J Climatol 6:293–335

Rowell DP (1997) Assessing potential seasonal predictability with an ensemble of multi-decadal ECM simulations. J Climate (in press)

Simmonds I, Budd WF (1991) Sensitivity of the southern hemisphere circulation to leads in the Antarctic pack ice. Q J R Meteorol Soc 117:1003–1024

Tett SFB, Johns TC, Mitchell JFB (1997) Global and regional variability in a coupled AOGCM. Clim Dyn (in press)

Trenberth KE (1976) Spatial and temporal variations of the Southern Oscillation. Mon Weather Rev 102:639–653

Trenberth KE (1985) Observed southern hemisphere eddy statistics at 500 mb: frequency and spatial dependence. J Atmos Sci 38:2585

Tzeng RY, Bromwich DH, Parish TR, Chen B (1994) NCAR CCM2 simulation of the modern Antarctic climate. J Geophys Res 99:23131–23148

van Loon H, Shea DJ (1987) The Southern Oscillation. Part VI: anomalies of sea level pressure on the southern hemisphere and of Pacific sea surface temperatures during the development of a warm event. Mon Weather Rev 115:370–379

van Loon H, Kidson JW, Mullan AB (1993) Changes in the semi-annual cycle in the Australian data set. In: Preprints, 4th Int Conf on Southern Hemisphere Meteorology and Oceanography. AMS, Hobart, pp 173–174